Experimental investigation of high-frequency noise and optical feedback effects using a 9.7 μm continuous-wave distributed-feedback quantum-cascade laser

Damien Weidmann, Kevin Smith, and Brian Ellison

An experimental investigation of high-frequency noise, i.e., up to 3 GHz, exhibited by a 9.7 μm quantum cascade laser, is described. Noise characteristics and measurements of a liquid-nitrogen-cooled continuous-wave distributed-feedback laser are presented. Well defined sets of narrow and intense resonance peaks have been observed in the 10–300 MHz range. Measurements of relative intensity noise have been performed. It is also shown that quantum-cascade lasers are sensitive to optical feedback. The excess noise generated by the feedback has been investigated under well defined conditions. A description of the experimental phenomenon is presented along with methods of minimizing optical feedback. © 2007 Optical Society of America

OCIS codes: 140.5960, 140.3600, 270.2500.

1. Introduction

Since their initial experimental demonstration,[1] mid-IR quantum cascade lasers (QCLs) have become a widely used continuously tunable laser source spanning applications from high-resolution molecular spectroscopy to optical communications. Because of the unipolar nature of the laser transition occurring in QCLs, they can be modulated at high frequencies, up to the gigahertz range. As high-frequency laser noise may impede performance of QCL-based systems, it is interesting to investigate high-frequency intrinsic laser-noise characteristics. Laser noise may be the dominant noise source in spectrometers based on frequency modulation detection schemes,[2] in optical heterodyne systems,[3] or in laser systems for free space communications using an optical link.[4]

Semiconductor laser-noise properties are usually affected by optical feedback (OF), primarily because of their short cavity length. Intensity and phase noise increase or reduction, power modulation, laser locking, optical bistability, and mode hopping are all OF-related phenomenon observed with semiconductor lasers. Depending on the purpose of the QCL-based system, an understanding of OF may help to minimize undesirable effects or even allow them to be exploited. Thus strategies to limit the amount of laser excess noise injected within the instrument can be developed.

The paper is organized as follows: the experimental details of the setup are first introduced. Noise spectra are then presented along with results from relative intensity noise (RIN) measurements. The last section before the conclusion describes an experimental investigation of OF effects on a QCL.

2. Experiment

A. Setup

The laser investigated during this work is a liquid-nitrogen-cooled distributed-feedback (DFB) QCL operating in the continuous-wave mode (cw) with a central wavelength at 9.7 μm. The laser ridge is 27 μm wide, 1.5 mm long (hereafter the cavity optical length is denoted L). The multi-quantum-well structure is a bound-to-continuum design comprising 35 cascade stages, as described in Ref. 5. The laser was installed in a liquid-nitrogen cryostat with a temperature control better than 1 mK. The injection current is supplied by a low-noise current source (noise and ripple below 10 μA).

Figure 1 is a schematic of the optical configuration. Laser radiation exits through a wedged barium fluo-

The authors are with the CCLRC Rutherford Appleton Laboratory, Space Science and Technology Department, Chilton, Didcot, Oxfordshire, OX11 0QX, UK. D. Weidmann can be reached by e-mail at d.weidmann@rl.ac.uk.

Received 14 August 2006; accepted 24 November 2006; posted 29 November 2006 (Doc. ID 74060); published 2 February 2007.
0003-6935/07/060947-07$15.00/0

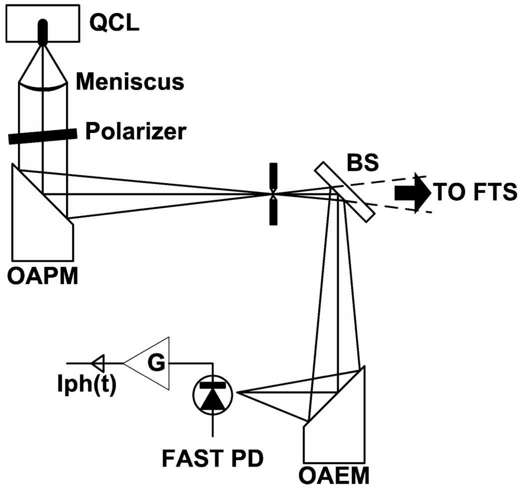

Fig. 1. Schematic of the optical configuration for high-frequency QCL noise measurements. OAPM, OAEM, BS, FTS, and PD are off-axis paraboloidal mirror, off-axis ellipsoidal mirror, beam splitter, Fourier transform spectrometer, and photodiode, respectively.

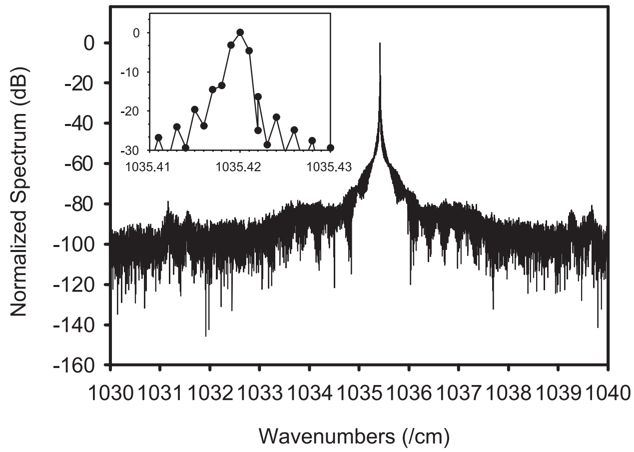

Fig. 2. Intensity-normalized spectrum of QCL emission recorded with a Bruker IFS 125HR Fourier transform spectrometer. The inset plot shows the −3 dB linewidth corresponding to the FTS resolution, the contribution from the laser linewidth being insignificant.

ride window and is collimated by a custom designed 12.5 mm diameter ZnSe aspheric meniscus with antireflection (AR) coating on both surfaces. The meniscus is opened at $F/\#0.5$ to ensure full collection of the highly divergent QCL beam. An intermediate image is formed by a 90° off-axis paraboloid (101.6 mm focal length). This intermediate image was included for beam manipulation purposes, for example, spatial filtering or amplitude modulation by a mechanical chopper. The beam is split into two parts by a 50/50 ZnSe beam splitter. The transmitted beam is reserved for characterization purposes, including power measurements and injection into a Fourier transform spectrometer. The reflected part is focused on a fast mercury cadmium tellurium (MCT) photodiode by a 90° off-axis ellipsoid (79.06 mm focal length). The detector used during this work was a 100 μm $\times$ 100 μm resonant optical cavity (ROC) MCT detector, exhibiting a 1.8 GHz 3 dB bandwidth and a 6 dB bandwidth over 3 GHz. The ROC has been designed for peak sensitivity at 9.7 μm. The DC part of the photocurrent is used for optical alignment and indirect power monitoring using an oscilloscope. The high-frequency part of the photocurrent is fed into a 35 dB gain, 3 GHz bandwidth preamplifier. The radio frequency (RF) power contained in the signal is detected by a Schottky diode, or the signal is fed into a RF spectrum analyzer.

B. Laser Specifications

QCL spectral characteristics were investigated using a Bruker IFS 125HR Fourier transform spectrometer (FTS) with a 6 m optical path difference. Figure 2 shows an intensity-normalized spectrum recorded at the maximum unapodized resolution, i.e., 0.0017 cm^{-1} (50 MHz). The spectrum indicates that the laser was operating in a single mode. At threshold (92 K, 650 mA) the laser emited at 1035.85 cm^{-1}. At higher current and temperature (1.12 A, 140 K) the laser frequency decreased to 1025 cm^{-1}. The maximum output power was approximately 35 mW. Current and temperature tuning rates were measured to be $-3.9\ cm^{-1}A^{-1}$ and $-0.065\ cm^{-1}K^{-1}$.

The spectral resolution of the FTS was insufficient to provide an estimation of the laser linewidth. To estimate this parameter, we performed tunable absorption spectroscopy over a low-pressure carbonyl sulfide (OCS) absorption line, the $P30$ transition located at 1035.4232 cm^{-1}.[6] A 52 mm long glass cell was filled with 0.072 mbar of pure OCS. At such low pressures the linewidth is determined solely by Doppler broadening, and the absorption profile should exhibit a full width at half-maximum (FWHM) of 49.5 MHz at 295 K.

Figure 3 shows the measured FWHM of the absorption line was 45 $\pm$ 3 MHz. As a first approximation the observed FWHM, $\Delta\nu$ is given by the convolution of the Doppler-broadened OCS line (FWHM α_D) and the Gaussian lineshape (FWHM $\Delta\nu_L$) of the laser emission:

$$\Delta\nu^2 = \alpha_D{}^2 + \Delta\nu_L{}^2, \qquad (1)$$

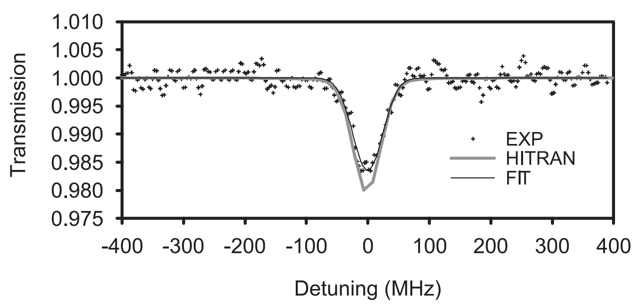

Fig. 3. Transmission spectrum of the Doppler-broadened P30 OCS absorption line at room temperature and 0.072 mbar total pressure.

as experimentally $\Delta\nu \approx \alpha_D$, which means $\Delta\nu_L^2 \ll \alpha_D^2$, or $10\Delta\nu_L^2 < \alpha_D^2$. Hence the laser linewidth is below 16 MHz, most likely close to the 1 MHz range, as already reported for free running QCLs operating at similar wavelengths.[7] Using active stabilization techniques, reduction of linewidth down to the kilohertz range has been reported.[8]

The long-term frequency stability was also observed by monitoring the variation of the acquired peak position of the OCS absorption line with time. A slow drift of 7 MHz over 30 minutes was observed, due to residual temperature variations.

The beam quality and alignment were verified and optimized using an IR thermal imager.

3. Intrinsic Noise

To perform measurements of the laser noise in the 0–3 GHz range, a mechanical chopper running at 1.78 kHz was introduced at the intermediate focus created by the off-axis parabolic mirror (OAPM). The preamplifier output was connected to a 0.01–12 GHz spectrum analyzer. The Y channel output of the analyzer was fed into a lock-in amplifier for synchronous demodulation. This method ensured that only the laser noise was taken into consideration.

Initially, 2 GHz wide spectra were recorded with a resolution of 300 kHz, as shown in Fig. 4. The 2–3 GHz frequency range was found not to exhibit any specific noise features. Unlike intraband semiconductor lasers, QCLs do not exhibit a photon–electron resonance peak around 1 GHz. In addition to the normal $1/f$ noise, clearly identified structures can be seen at frequencies up to 300 MHz. The most intense of these occur below 200 MHz, as shown in Fig. 5. These peaks are very intense: between 10 and 20 dB above the noise floor, and sharp. The inset of Fig. 4 shows the spectral record of a single peak at 83 MHz, obtained with a 3 kHz resolution bandwidth. The peak exhibits a FWHM of about 10 kHz, yielding a resonance with a quality factor of around 8000.

Figure 5 shows noise spectra, recorded at 300 kHz resolution, but limited this time to the 0–200 MHz

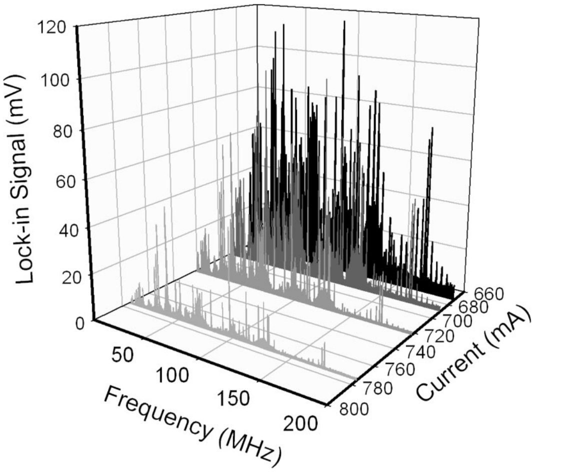

Fig. 5. Noise spectra recorded in the 0–200 MHz region for four different injection currents.

region. Spectra for four different injection currents were recorded: 672.6, 689.6, 721.9, and 775.2 mA. For these measurements a wire-grid polarizer was inserted into the beam and adjusted so that the power measured at the detector remained constant. The expected decrease in laser noise with injection current was observed.

The spectrum analyzer output (dBm) was then converted to relative intensity noise (RIN). The mechanical chopper and lock-in amplifier were removed to perform noise within the full measurement line. The detector and the RF line were fully shielded with a 100 dB attenuation shielding material. The AC component of the RIN is given by

$$\mathrm{RIN}(f) = \frac{1}{I_{\mathrm{ph}}^{2}}\left[\frac{10^{X(f)/10}}{G^2 \times R \times \Delta f \times 1000}\right], \tag{2}$$

where $X(f)$ are the spectrum analyzer signals in decibels, G is the amplification gain, R is the load impedance, Δf is the analysis bandwidth, and I_{ph} is the measured photocurrent.

Four frequencies were chosen to investigate the RIN variation with injection current and output power: 200, 500, 1000, and 2000 MHz, respectively. The results are plotted in Fig. 6. The contribution from thermal noise and shot noise is also plotted. This

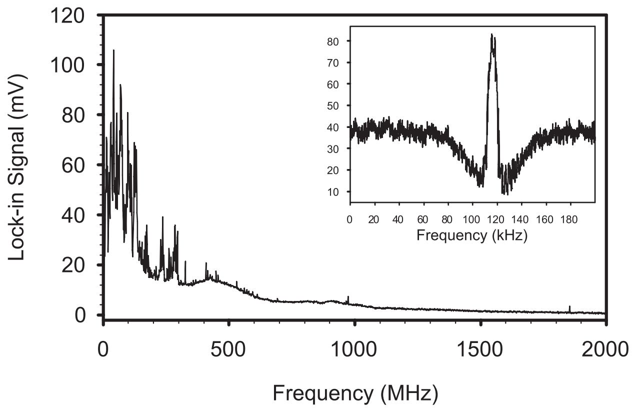

Fig. 4. 2 GHz wide spectrum of the high-frequency component of the photocurrent under laser illumination. The resolution bandwidth was 300 kHz. The inset shows a well defined resonance peak at 83 MHz recorded at 3 kHz resolution.

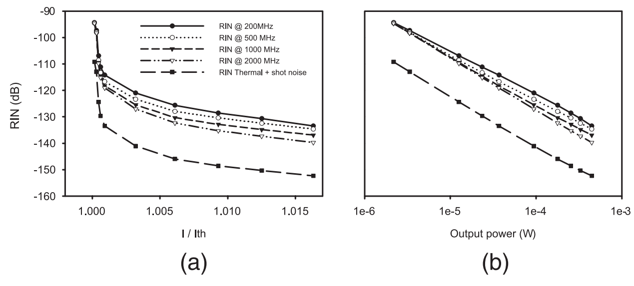

Fig. 6. RIN measurements versus injection current and optical power, performed at four different frequencies.

contribution was calculated from

$$\mathrm{RIN}_{\mathrm{Th+sn}} = \frac{1}{I_{\mathrm{ph}}{}^2}\left(\frac{4k_{\mathrm{B}} \times T}{R} + 2 \times e \times I_{\mathrm{Ph}}\right), \tag{3}$$

where T is the noise temperature of the amplifier (102 K).

As expected, and as observed with interband semiconductor lasers, the RIN is proportional to the laser output power raised to the scaling parameter exponent: $P^{-\gamma}$. Rana *et al.* and Gentsy *et al.* have recently published semiclassical models of QCL noise describing the RIN behavior.[9,10] Gentsy *et al.* have reported γ values in the range of 2.1 for a 25-stage laser device.[11] From the data recorded during this study, the scaling factor γ was observed to increase slightly as the frequency increases: 1.67, 1.72, 1.83, and 1.96 for 200, 500, 1000, and 2000 MHz, respectively. These values are smaller than those given in Ref. 11, which is consistent as the QCL used in this work has 35 cascade stages. A much smaller scaling factor of 1.1 was measured for the noise peak at 83 MHz.

4. Optical Feedback

Spurious OF can have a profound effect on semiconductor lasers operating in the cw mode.[12,13] Depending on the feedback conditions, effects such as laser line broadening, mode hops, and generation of excess low- and high-frequency noise may degrade the laser performance. Conversely, when the OF is controlled, phase and intensity noise reduction in the laser emission can be achieved. OF effects on telecom laser diodes and also lead salt lasers have been widely studied.[14–17]

In most applications, OF is not controlled, and it occurs due to unwanted reflections from optical components in the system. The feedback is then weak. Usually laser linewidth is not strongly affected under weak feedback conditions, and the effect on systems such as tunable diode laser spectrometers will be residual etalon fringes. This may limit the sensitivity of the spectrometer if fringes are of similar strength to the absorption signal. However, in applications where photomixing and coherent detection are involved, like homodyne and heterodyne systems, the mode mixing introduced by OF may be a severely limiting factor.[18]

Continuous-wave DFB QCLs are likely to be particularly sensitive to OF because of the following:

- They exhibit a very good spectral purity (long photon lifetime).
- They are short cavity lasers (though 4 to 5 times longer than telecommunications or lead salt devices).

To first order, the optical feedback is likely to perturb the laser behavior providing that the reinjected fraction of power f_{EXT} is such that[12]

$$f_{\mathrm{EXT}} \gg \left(\frac{\Delta f}{\Delta \nu}\right)^2, \tag{4}$$

where Δf is the laser linewidth and $\Delta\nu$ is the longitudinal mode spacing. For a typical cw QCL, if we consider a 5 MHz laser linewidth and a 2 mm long cavity, it follows that a fraction of reinjected light much greater than -70 dB will affect the QCL's behavior. Also, since the coherence length is on the scale of hundreds of meters, reflections from very distant objects are relevant.

The optical configuration shown in Fig. 1 has been designed to optimally reduce OF. By use of off-axis reflective optics, feedback-free and optimal alignment can be achieved. The only transmitting optical component in the path is the ZnSe collimating meniscus. The AR coatings on the meniscus have been measured to transmit 98.5% of radiation at the working wavelength. The potential effect of the reflected radiation was investigated by running a simulation with ray-tracing software (Zemax). Calculations show that for perfect alignment, the fraction of light reinjected would be -67 dB. The sensitivity of this fraction with respect to lens tilt (+/− 1–2 degrees) and position along the optical axis (+/− 10% of the effective focal length) was found to be insignificant. Therefore we conclude that no significant OF was introduced by the collimating meniscus.

Whatever the optical configuration of an instrument, at some point the radiation is incident on a detector. If perfectly aligned, the surface of the detector acts as an autocollimated partial reflector. The use of a ROC introduces more OF than would be expected from a conventional MCT detector. The ROC has been fine tuned to the precise working wavelength by addition of an uncoated germanium layer. Consequently, the feedback introduced by a perfectly aligned detector chip is expected to be 18%, considering the refractive index of Ge and the BS present in the path. This feedback level is far more than -70 dB and should strongly affect the QCL lasing properties. Unlike many previous studies[14–17] on OF in semiconductor lasers, the weak feedback approximation can no longer be made. Small-signal analysis applied to the linearized rate equations is no longer valid. Reference 19 provides a full numerical solution of the rate equations applicable for a high level of feedback.

The presence of standing waves between the laser source and the detector was first investigated by moving the detector itself. The effect on the measured power is plotted in Fig. 7. The results are not indicative of a standing wave; rather, the observed power variation indicates that the laser was being successively locked to extended cavity modes. The slowly decreasing envelope stems from defocusing of the beam. The length L_{ext} of the extended cavity formed is 49.7 cm, approximately 200 times the length of the laser cavity. The spatial separation between two consecutive extended cavity modes derived from Fig. 8 is 5.0 ± 0.2 μm. This corresponds to laser emission at $1000 \pm 40\ \mathrm{cm}^{-1}$, which is consistent with the actual laser operating frequency of $1035.55\ \mathrm{cm}^{-1}$.

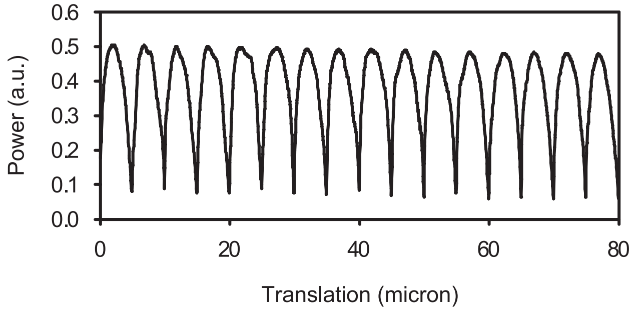

Fig. 7. Laser power modulation observed while translating the detector along the optical axis.

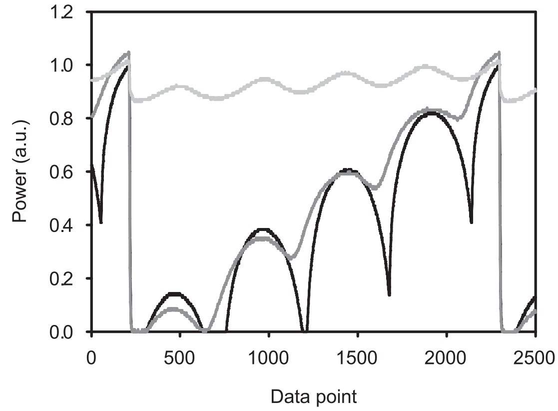

(a)

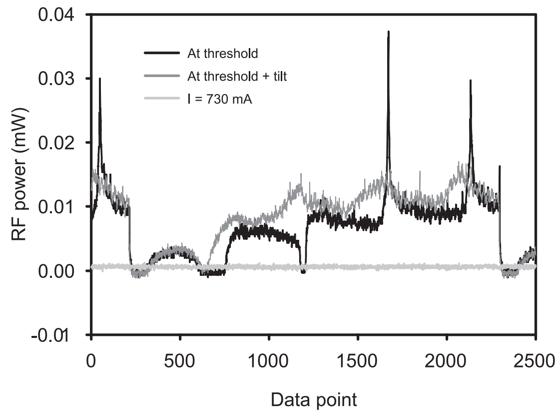

(b)

Fig. 8. (a) Effect of the OF during a 10 mA current scan. (b) Corresponding recording of the RF power within the detector bandwidth showing noise peaks correlated to the switching from one extended cavity mode to another.

It is worth noting that under such strong OF conditions, maintaining the stability of the laser power becomes critical. The slightest change in extended cavity length produces significant power modulation. The refractive index of air changes at a rate of 10^{-6} per degree Kelvin, and the thermal expansion of the optical table steel is 10 ppm per degree. High temperature stability is then required to avoid power-level drifts.

Considering the description from Ref. 19, the feedback coefficient C is given by

$$C = \frac{L_{\text{ext}}}{n \times L} \frac{1-R}{\sqrt{R}} \sqrt{f_{\text{EXT}}}, \tag{5}$$

which yields $C = 60$ using $n = 3.2$ for the intracavity refractive index. R is the laser facet reflectivity. Not surprisingly, the feedback regime is strong. For conventional semiconductor lasers, the expression of C should include the contribution from the linewidth enhancement parameter α, which is proportional to the variation of the refractive index with the carrier injection. For a QCL this parameter was thought to be essentially zero.[1] Recent measurements show that α varies with the injection current, and values from -0.5 to 2 were reported.[20] A α parameter close to zero has a profound effect on the laser behavior under the strong feedback regime since the coherence collapse cannot occur. Based on the definition of the different feedback regimes of Ref. 19, a QCL with $\alpha \cong 0$ can never operate in regime IV but will remain in regime III, where it is locked on the extended cavity mode and exhibits a significant line narrowing.

Figure 8(a) shows measured laser output power while applying a 10 mA current ramp to the laser, corresponding to a spectral scan of 3.9×10^{-2} cm^{-1}. The influence of OF is obvious; rather than a linear increase of power with current (as given with a thermopile), one can see a strong amplitude modulation corresponding to the laser being "forced" to operate in extended cavity modes. Three different cases are shown: (1) with the detector well aligned and the laser operating near threshold, (2) with a 5 degree tilt in the detector alignment and the laser operating near threshold, and (3) with the detector well aligned and the laser operating at 100 mA above threshold.

Also, Fig. 8(b) shows the corresponding RF power within the full bandwidth of the detector during the current scan. Between peaks 1 and 2, and 2 and 3, the laser returns to below threshold, and hence the noise vanishes. Note that using extended cavity modes is a method to decrease the laser threshold slightly. Between lobes 3 and 4, and 4 and 5, we observed a sharp and intense peak of noise power. This is likely to correspond to a laser oscillation between the two neighboring extended cavity modes, with a relaxation frequency of between 120 and 180 MHz. This was observed with the spectrum analyzer when operating the laser between two extended cavity modes. It is worth noting that tilting the detector does reduce the OF since the contrast observed on power modulation decreases. However, whatever the operating conditions of the laser, tilting the detector always results in RF noise enhancement; hence this is not the ideal solution to obviate OF when low-noise operation is required.

At higher current, a form of saturation occurs, and the seed from the distant reflector is not as efficient. The measured power corresponds to a weak feedback level, and only etalon modulation remains. This corresponds to a shift toward higher values of the feedback coefficient, the operating mode transiting from regime II to III, as defined in Ref. 19. At the same

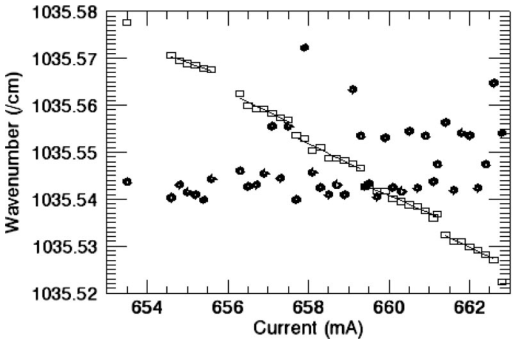

Fig. 9. Evolution of the peak position (left scale) and the FWHM (right scale) of the laser emission spectrum with the injection current, starting from threshold. Transitions from one extended mode to another correspond to a visible step in frequency and in a significant increase of the FWHM in three occasions.

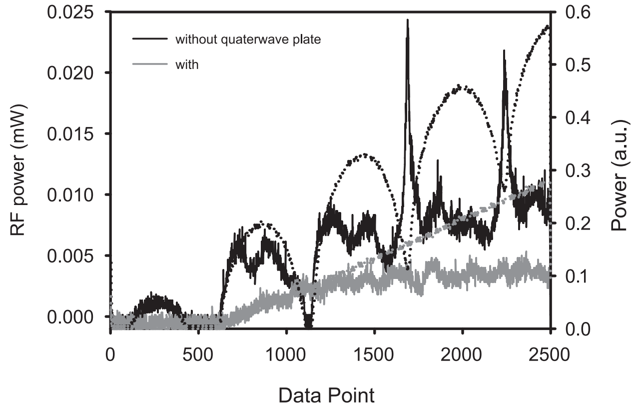

Fig. 10. Plot similar to Fig. 8, showing the effectiveness of the quarter-wave plate in suppressing OF.

time, as described in the previous section, the RIN is reduced with increased output power, and the RF power level is considerably reduced.

The spectral behavior under strong OF was further investigated by coupling the transmitted part of the laser power with the Bruker IFS 125HR FTS. The laser current was scanned from threshold ($T = 94$ K, $I = 653.5$ mA) up to $I = 662.8$ mA with 0.2 mA steps. At each of the steps a 0.01 cm^{-1} resolution spectrum was recorded to accurately determine the emission frequency. Figure 9 shows a plot from this data set. It shows the laser frequency as a function of current. Rather than a continuous tuning, steps are observed that are coincident with drops in power between two extended cavity modes. This is due to the sudden hop from one of the extended cavity modes to the next one. The theoretical free spectral range of the extended cavity is 0.010 cm^{-1}. Assuming that the central point of each segment in Fig. 9 corresponds to the peak power emission within the given extended cavity mode, the free spectral range was found to be consistent with the theoretical value.

Due to the unstable nature of the laser emission when operating between two consecutive extended cavity modes, it was not possible to record high-resolution spectra of the corresponding emission with the FTS. A high-resolution FTS measurement requires a few minutes, but the unstable operation of the laser usually only lasts for a few seconds, as indicated by the apparition of a peak in the 120 to 180 MHz range on the spectrum analyzer. However, in Fig. 9 there are three anomalous increases in the FWHM of the emission spectrum corresponding to a transition between two extended cavity modes. The lineshape was also observed to have an unusual triangular shape.

Several methods of reducing feedback have been investigated. Tilting the detector did not appear to be a suitable solution since it reduced the power at the detector and did not prevent RF noise enhancement, as witnessed by Fig. 8.

The introduction of pinholes has also been tried unsuccessfully. Though machined with a conical profile, they introduced their own OF that perturbed the laser.

Of the methods investigated during this work, the best was the introduction of a quarter-wave plate before the detector. Reflection from the detector chip introduces a π phase shift, and a polarizer could then be used to block the backreflected radiation. The polarizer extinction ratio was 1/300, and Fig. 10 shows the observed suppression of feedback. Once the orientation of the quarter-wave plate had been optimized, the amplitude modulation due to OF vanished, and the residual amplitude modulation of the laser power was decreased to 0.1%. We have also measured a similar amount of RF power when reducing the detection bandwidth to 200 MHz, showing that the OF induced noise remains within that band and is insignificant at higher frequencies. A more efficient way of reducing OF would be the introduction of a dedicated Faraday isolator,[21] with a higher extinction ratio.

5. Conclusion

We have presented an experimental investigation of the intrinsic and OF-related high-frequency noise in a cw DFB QCL. The scaling parameters deduced were in good agreement with those observed previously[11] for a different QCL device. Within the noise spectrum, a series of intense sharp peaks have been observed, mainly in the 0–200 MHz range. These peaks have a much smaller scaling parameter, around 1.1. OF effects have also been characterized. As expected, under strong OF, no coherence collapse regime was observed. The use of a quarter-wave plate–polarizer system was found to be the most efficient isolation technique. It is worth noting that, even though this work emphasizes the use of a ROC detector, conventional detectors (MCT with AR coating) and immersed lens technology detectors have been observed to show similar behavior.

OF may not always be a problem, since it could be used under controlled conditions to lock laser frequencies. Considerable linewidth reduction, up to the kilohertz range, would also be expected.

The authors wish to thank Gary Williams and Brian Landowsky from the Space Science and Technology Department of the Rutherford Appleton Laboratory (RAL) for their technical support. The Engineering and Physical Science Research Council instruments loan pool is also acknowledged for provision of a thermal imaging system. This work was supported by the Natural Environment Research Council (grant NER/Z/S/2003/00642) and the Earth Observation and Atmospheric Science Division of RAL.

References

1. J. Faist, F. Capasso, D. L. Sivco, C. Sirtori, A. L. Hutchinson, and A. Y. Cho, "Quantum cascade lasers," Science **264,** 553–556 (1994).
2. J. A. Silver, "Frequency modulation spectroscopy for trace species detection: theory and comparison among experimental methods," Appl. Opt. **31,** 707–717 (1992).
3. G. Sonnabend, D. Wirtz, and R. Schieder, "Evaluation of quantum-cascade lasers as local oscillators for infrared heterodyne spectroscopy," Appl. Opt. **44,** 7170–7173 (2005).
4. R. Martini, R. Paiella, C. Gmachl, F. Capasso, E. A. Whittaker, H. C. Liu, H. Y. Hwang, D. L. Sivco, J. N. Baillargeon, and A. Y. Cho, "High-speed digital data transmission using mid-infrared quantum cascade lasers," Electron. Lett. **37,** 1290–1292 (2001).
5. R. Maulini, M. Beck, J. Faist, and E. Gini, "Broadband tuning of external cavity bound-to-continuum quantum-cascade lasers," Appl. Phys. Lett. **84,** 1659–1661 (2005).
6. L. S. Rothman, D. Jacquemart, A. Barbe, D. Chris Benner, M. Birk, L. R. Brown, M. R. Carleer, C. Chackerian, K. Chance, L. H. Coudert, V. Dana, V. M. Devi, J.-M. Flaud, R. R. Gamache, A. Goldman, J.-M. Hartmann, K. W. Jucks, A. G. Maki, J.-Y. Mandin, S. T. Massie, J. Orphal, A. Perrin, C. P. Rinsland, M. A. H. Smith, J. Tennyson, R. N. Tolchenov, R. A. Toth, J. Vander Auwera, P. Varanasi, and G. Wagner, "The HITRAN 2004 molecular spectroscopic database," J. Quant. Spectrosc. Radiat. Transfer **96,** 139–204 (2005).
7. D. Weidmann, L. Joly, V. Parpillon, D. Courtois, Y. Bonetti, T. Aellen, M. Beck, J. Faist, and D. Hofstetter, "Free-running 9.1-mm distributed-feedback quantum cascade laser linewidth measurement by heterodyning with a $C_{18}O_2$ laser," Opt. Lett. **28,** 704–706 (2003).
8. R. M. Williams, J. F. Kelly, J. S. Hartman, S. W. Sharpe, M. S. Taubman, J. L. Hall, F. Capasso, C. Gmachl, D. L. Sivco, J. N. Baillargeon, and A. Y. Cho, "Kilohertz linewidth from frequency-stabilized mid-infrared quantum cascade lasers," Opt. Lett. **24,** 1844–1846 (1999).
9. F. Rana and R. J. Ram, "Current noise and photon noise in quantum cascade lasers," Phys. Rev. B **65,** 125313 (2002).
10. T. Gentsy and W. Elsäßer, "Semiclassical model for the relative intensity noise of intersubband quantum cascade lasers," Opt. Commun. **256,** 171–183 (2005).
11. T. Gensty, W. Elsäßer, and C. Mann, "Intensity noise properties of quantum cascade lasers," Opt. Express **13,** 2032–2039 (2005).
12. G. P. Agrawal and N. K. Dutta, *Long-Wavelength Semiconductor Lasers* (Van Nostrand Reinhold, 1986).
13. K. Petermann, *Laser Diode Modulation and Noise* (Kluwer Academic, 1991).
14. L. Goldberg, H. F. Taylor, A. Dandridge, J. F. Weller, and R. O. Miles, "Spectral characteristics of semiconductor lasers with optical feedback," IEEE J. Quantum Electron. **18,** 555–563 (1982).
15. J. Henrik and N. Gade, "Influence of optical feedback on laser frequency spectrum and threshold conditions," IEEE J. Quantum Electron. **19,** 465–469 (1983).
16. P. Spano, S. Piazzolla, and M. Tamburrini, "Theory of noise in semiconductor lasers in the presence of optical feedback," IEEE J. Quantum Electron. **20,** 350–357 (1984).
17. C. H. Henry and R. F. Kazarinov, "Instability of semiconductor lasers due to optical feedback from distant reflectors," IEEE J. Quantum Electron. **22,** 294–301 (1986).
18. C. N. Harward and J. M. Hoell, "Optical feedback effects on the performance of $Pb_{1-x}Sn_xSe$ semiconductor lasers," Appl. Opt. **18,** 3978–3983 (1979).
19. N. Schunk and K. Petermann, "Numerical analysis of the feedback regimes for a single mode semiconductor laser with external feedback," IEEE J. Quantum Electron. **24,** 1242–1247 (1988).
20. J. von Staden, T. Gentsy, W. Elsäßer, G. Giuliani, and C. Mann, "Measurements of the a-factor of a DFB-quantum cascade laser by a novel feedback self-mixing technique," Opt. Lett. **31,** 2574–2576 (2006).
21. M. S. Taubman, T. L. Myers, B. D. Cannon, and R. M. Williams, "Stabilization, injection and control of quantum cascade lasers, and their application to chemical sensing in the infrared," Spectrochim. Acta A **60,** 3457–3468 (2004).